Denoising of Hyperspectral Signal from Drone for *Ganoderma* Disease Detection in Oil Palm

Izzuddin, M. A.,[1] Hamzah, A.,[2] Nisfariza, M. N.,[3] Idris, A.S.,[1] Nor Aizam, A.,[4*] Sharul Aikal, B. M.,[4] Nordiana, A. A.,[1] Mohd Najib, A.[1] and Mohd Shukri, I.[1]
[1]Malaysian Palm Oil Board (MPOB), No.6, Persiaran Institusi, Bandar Baru Bangi, 43000 Kajang, Selangor, Malaysia, E-mail: mohamad.izzuddin@mpob.gov.my, idris@mpob.gov.my, nordiana@mpob.gov.my, mnajib@mpob.gov.my, mohd.shukri@mpob.gov.my
[2]Department of Electrical Engineering, Faculty of Engineering, University of Malaya, 50603 Kuala Lumpur, Malaysia, E-mail: ahamzah@um.edu.my
[3]Department of Geography, Faculty of Arts and Social Sciences, University of Malaya, 50603 Kuala Lumpur, Malaysia, E-mail: nish@um.edu.my
[4]School of Geomatics Science and Natural Resources, College of Built Environment, Universiti Teknologi MARA, Shah Alam, Selangor Darul Ehsan, Malaysia
E-mail: nor_aizam@uitm.edu.my*, shahhhaikal95@gmail.com
**Corresponding Author*

DOI: https://doi.org/10.52939/ijg.v19i5.2659

Abstract

Oil palm is an important crop that generates high income to Malaysia. However, the oil palm is susceptible to Ganoderma *infection that reduces the productivity of the oil palm. Conventional ground-based disease detection is laborious and costly. Therefore, airborne remote sensing technology coupled with ground detection provides a more effective control of the disease. Airborne hyperspectral remote sensing utilizes narrow and contiguous bands to assist in detection of diseases in crops. Spectral responses recorded by the camera tend to suffer from interference and these noises could reduce the quality of the data. Therefore, this study presents the application of Savitzky-Golay and wavelet spectral denoising technique to improve the hyperspectral signatures for* Ganoderma *disease detection in oil palm.*

Keywords: Denoising, *Ganoderma*, Hyperspectral, Oil Palm

1. Introduction

Oil palm is one of the main commodities in Malaysia and provides high income to the country. In 2021, Malaysia had produced about 18 million tonnes of CPO. Total export of oil palm products in 2021 valued at RM108.52 billion [1]. Like most crops, the oil palm can be devastated by diseases and one of them is caused by the fungus, *Ganoderma boninense*. The *Ganoderma* related disease can cause income losses of up to RM 1.5 billion per year [2]. Several ground and lab-based *Ganoderma* disease detection technologies have been developed by the Malaysian Palm Oil Board (MPOB) namely Ganosken Tomography [3], Polymerase Chain Reaction- Deoxyribonucleic Acid (PCR-DNA) analysis [4] and *Ganoderma* Selective Medium (GSM) [5]. These technologies require in-field inspection of individual palms as well as tissue sampling which are time consuming, laborious and costly. The availability of lightweight hyperspectral drones offers opportunities for aerial detection of *Ganoderma* disease in oil palm. The aerial detection approach can be used to assist in the implementation of ground and lab-based technologies to validate the presence of *Ganoderma* disease in the field. Prior to this, ground-based hyperspectral studies using field spectroscopy have been carried out by the Malaysian Palm Oil Board (MPOB) using field spectroradiometer GER1500 for *Ganoderma* disease detection in oil palm seedlings [6] and [7].

Spectral signatures from healthy and *Ganoderma*-infected oil palm were successfully identified in previous studies [6] and [7]. However, due to noise interference, spectral signatures from the airborne hyperspectral images were relatively different from those captured via field spectroscopy. Hence, there is a need to denoise the spectral from the airborne hyperspectral image for it to be similar to the field spectroscopy spectral signatures, that would then lead to an enhanced discriminating power between healthy and *Ganoderma*-infected oil palms.

The noises in the hyperspectral image usually originate from the change in the sun's illumination during image acquisition. High amount of cloud cover increases humidity in the field causing distortion to water-sensitive wavelengths that result in spectral noises over the respective spectrum region. These noises tend to reduce spectral separability between features due to overlapping spectrums whereby oil palm foliar is masked by high humidity as well as from other environmental factors such as cloud cover, different sun illumination intensity and reflectance from the soil background caused by intense sunny hot day. Therefore, there is a need to study and develop a denoising technique to cancel off interfering spectral signatures especially in warm and humid areas to obtain accurate readings for high accuracy classification. Shafri and Yusof [8] suggested wavelet-based denoising technique to denoise hyperspectral spectral signatures. Meanwhile Jardim and Morgado-Dias [9] suggested that Savitzky-Golay denoising technique also showed promising results in hyperspectral image denoising. Therefore, the objective of this study is to compare Savitzky-Golay and wavelet spectral denoising techniques for denoising spectral signatures from airborne hyperspectral images.

2. Materials and Methods

The flowchart of methodology is shown in Figure 1.

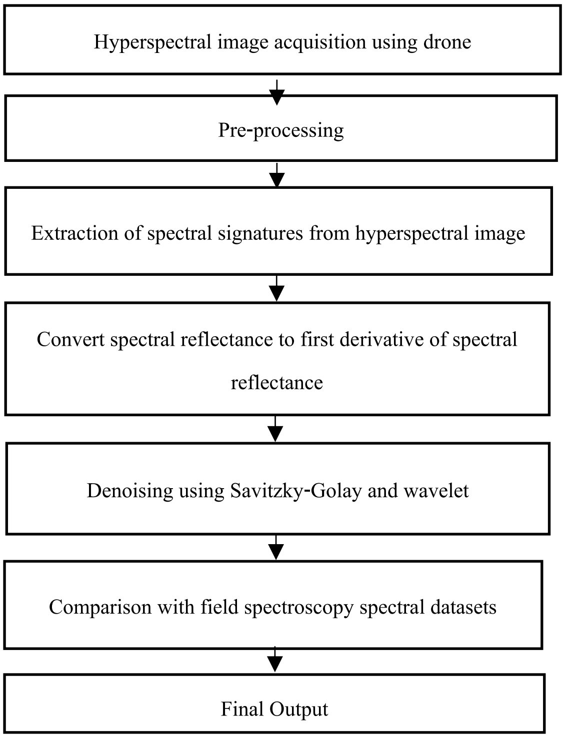

Figure 1: Flowchart of hyperspectral image analysis

2.1 Study Area

The study area is located in Lekir, Perak, Malaysia planted with Dura x Pisifera (DxP) at nine years of age. Its topography is categorised as flat coastal soil with good amount of annual rainfall (2701 mm). The area only has incidences of *Ganoderma* disease without any other known stresses or pest infestations reported.

2.2 Device and Equipments

The hyperspectral camera used was Resonon Pika L (Resonon Inc., Bozeman, Montana, USA) mounted on a DJI M600 Pro hexacopter drone. The camera captured an image with 300 spectral bands (350 nm – 100 nm) at ±2 nm spectral resolution. The drone was a hexacopter-type drone that can carry a maximum payload of 6 kg and a flight duration of 15 – 20 minutes. A calibration tarpaulin is also used as image white-calibration reference on the ground.

2.3 Ground Data Collection

The ground data collection was conducted during drone data acquisition in September 2019. The data consisted of census of healthy (H) and *Ganoderma* infected (I) oil palms. The description of healthy and *Ganoderma*-infected oil palm is shown in Table 1. The ground census was conducted by visual inspection of each individual palm in the field. The ground census data were recorded on paper sheets. The coordinate of the study area boundary was also recorded using a handheld Global Positioning System (GPS). Meanwhile, field spectroscopy data were collected using GER1500 field spectroradiometer. The spectral signatures were acquired from the foliar of frond number 9 and 17 from each of the H and I oil palms. Description of healthy and *Ganoderma*-infected oil palm.

2.4 Data Pre-Processing and Denoising

The ground census data were digitised for the Geographic Information System (GIS) database using ArcGIS 10.3.1 software. The data were saved in shapefile format. Subsequently, geometric and radiometric corrections were conducted on each of the raw hyperspectral image scanlines. The corrected image scanlines were then mosaiced into full scene images using Spectronon Pro software [10]. The individual bands of the corrected hyperspectral image were then checked for noise using visual inspection band by band through the image display window in ENVI 5.0 software. Through visual inspection, heavy speckle-like noise usually in the range of band 259 to 300 were removed resulting in a pre-processed image with 248 bands from 410 nm to 924 nm.

Table 1: Description of healthy and *Ganoderma*-infected oil palm

Label	Category	Description
	Healthy Oil Palm	Foliar looks healthy green, no lowering of older fronds and no presence of white mycelium, small white button, or fruiting bodies of *Ganoderma* or rotting at the stem base (GSM negative).
	Ganoderma-infected Oil Palm	Foliar symptoms may or may not exist, lowering of older fronds and confirmed presence of white mycelium, small white button, or fruiting bodies of *Ganoderma* or rotting at the stem base (GSM negative).

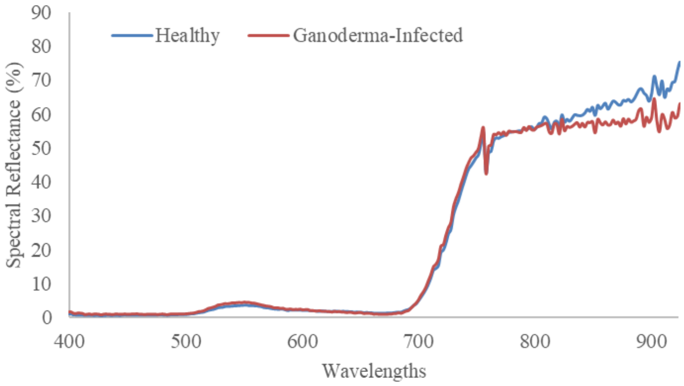

Figure 2: The average spectral signatures for healthy and *Ganoderma*-infected oil palm

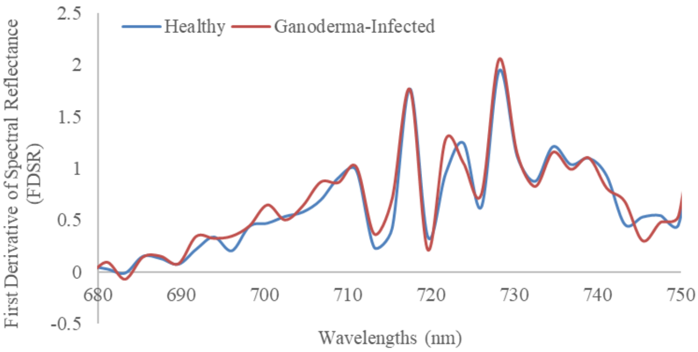

Figure 3: The first derivative of spectral signature for healthy and *Ganoderma*-infected oil palm before denoising

Through visual inspection, heavy speckle-like noise usually in the range of band 259 to 300 were removed resulting in a pre-processed image with 248 bands from 410 nm to 924 nm. Following that, the digitised ground census was overlaid onto the pre-processed hyperspectral image to allow identification of spectral signatures from healthy and *Ganoderma*-infected oil palms. For each of the categories, 50 spectral signatures were extracted and stored in the ASCII format. The average spectral signatures for H and I are plotted in Figure 2. The averaged spectral signatures in Figure 2 represent healthy and *Ganoderma*-infected oil palm prior to denoising. The spectral signatures showed a low magnitude of spectral reflectance values from 400 nm with minimal fluctuations observed from 500 to 700 nm. It was then followed by a steep climb from 700 nm to 800 nm along the red edge spectrum region with sudden spikes at 750 nm to 780 nm due to the noise. The spectral response continues to increase until 950 nm. Next, the spectral signatures were transformed to the first derivative spectral reflectance (FDSR) based on the method proposed by Izzuddin et al., [7] for inspection of random spike and valley-like noises that can be visually observed as shown in Figure 3.

3. Results and Discussion

The denoising process was conducted on the spectral signatures from both H and I FDSR datasets which were acquired from the hyperspectral image. The processed FDSR dataset from field spectroscopy is then used as a reference or benchmark for visual assessment of denoising output quality (Figure 4). The FDSR from field spectroscopy is used as reference for clean spectral signatures because the spectral measurement was conducted directly from the foliar using field spectroradiometer device directly in the field where source of noises is very limited. Meanwhile, Figure 5 is an example of raw FDSR spectral of H and I airborne hyperspectral image requiring denoising. The image represents spectral signatures of the oil palm canopy that have undergone pre-processing for geometry and radiometric corrections and mosaiced using the ENVI 5.0 classic software. ENVI 5.0 software can assist in image brightness and colour balancing during the mosaicking process. The raw FDSR of the H and I from airborne hyperspectral image were denoised using the wavelet technique suggested by Shafri and Yusof [8] and Savitzky-Golay data smoothing technique [9]. Both techniques have been built into MATLAB 2020a software.

For wavelet denoising, the mother wavelet Daubechis 9 using four level of decomposition as suggested by Shafri and Yusoff [8] was used. While, Savitzky-Golay denoising parameter employs the 2nd degree polynomial with a 5 frame length. The denoised airborne hyperspectral spectral signatures were compared with clean field spectroscopy as shown in Figure 6(a) - (c). Figure 6 showed that the spectral signatures denoised with Savitzky-Golay (Figure 6(b)) visually showed better similarity with field spectroscopy signatures compared to the wavelet-based denoised spectral signatures (Figure 6(a)). Thus, suggesting that, Savitzky-Golay technique is more suitable for use for denoising airborne hyperspectral images.

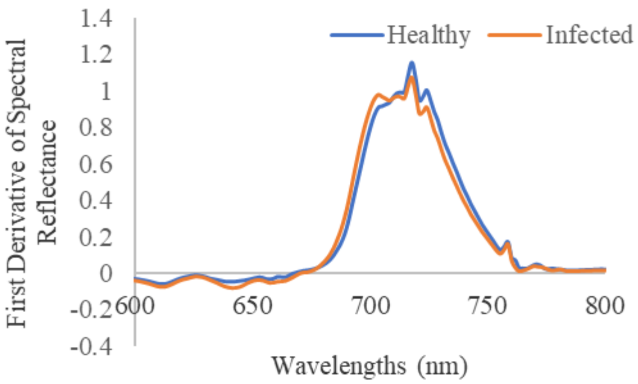

Figure 4: First derivative of spectral reflectance of healthy and *Ganoderma*-infected oil palm from field spectroscopy from 600 nm to 800 nm

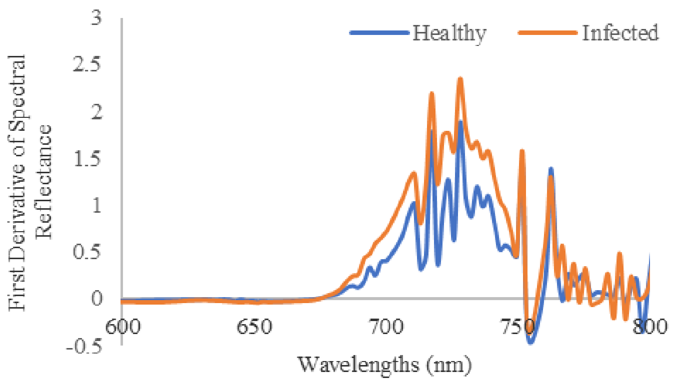

Figure 5: Raw first derivative of spectral reflectance of healthy and *Ganoderma*-infected oil palm from airborne hyperspectral from 600 nm to 800 nm

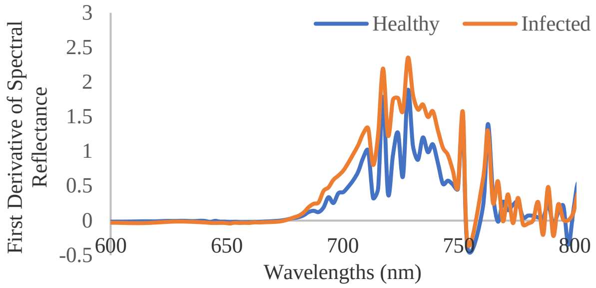

(a)

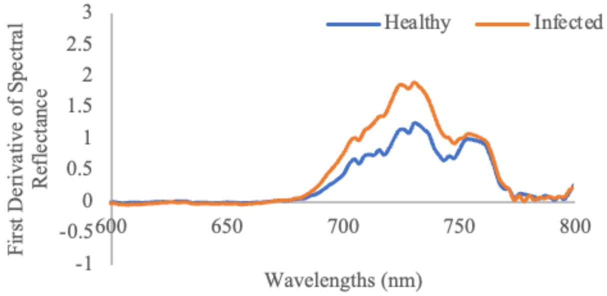

(b)

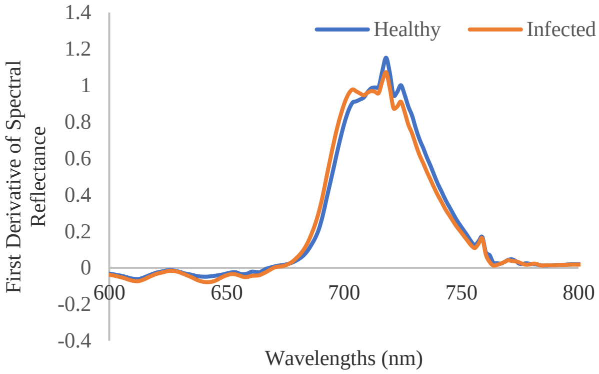

(c)

Figure 6: Comparison of denoised (a) wavelet (b) Savitzky-Golay spectral signatures (c) clean field spectroscopy spectral signatures

The denoising process is crucial to ensure that hyperspectral signatures of each oil palm agree with ground spectral signatures taken with the spectroradiometer. This latter portable field device is used to generate spectral readings directly using a halogen light-probe also known as a field spectroscopy technique. This apparatus allows pure spectral to be captured from oil palm leaflets without the noise from the changing sunlight illumination, humidity, and other environmental factors. The noises in the spectral signatures can be viewed and assessed in the form of FDSR. The FDSR calculates the slope between each spectral response from each narrow contiguous wavelength and then provides visualization of valleys and peaks indicating the magnitude of the spectral responses. The FDSR is important for assessment of the denoising quality using mean comparison with ground-based spectral signatures with low noises. Figure 6(a) showed that the raw spectral signatures contained noises that form jagged peaks and valleys visualized clearly from 600 nm to 800 nm of the FDSR datasets. After denoising, the spectral signatures in Figure 6(b) were largely smoothened showing only mild peaks and valleys especially from 700 to 750 nm. The denoised spectral signatures in Figure 6(b) share similar pattern with Figure 6(c) from the field spectroscopy of the oil palm foliar. The denoised spectral signatures from the airborne hyperspectral images seem to provide higher spectral responses with each increase in wavelength, compared to field spectroscopy signatures. The peaks in the 700 to 750 nm range have higher values and bigger shapes than the field spectroscopy signatures. These could be due to the enhancement of the data after the denoising process. The denoised spectral signatures can then be used as input for image classification using neural networks or other deep learning classifiers.

4. Conclusion and Recommendations

Airborne hyperspectral imagery tends to generate noise due to change in sunlight illumination and cloud cover during image acquisition. Therefore, denoising spectral signatures is important to remove interference and only extract clean spectral signatures from the features of the image. Our results showed that Savitzky-Golay denoising technique provides better processed spectral signatures compared to wavelet-based method. To develop a robust spectral denoising technique, different illumination will be investigated next.

Acknowledgement

Authors acknowledge the Ministry of Higher Education (MOHE) for funding under the Fundamental Research Grant Scheme (FRGS) (FRGS/1/2021/WAB04/UITM/02/2). We would like to acknowledge the officers and support staff of Malaysian Palm Oil Board (MPOB), University of Malaya (UM) and Universiti Teknologi MARA (UiTM) that assisted us to with providing the funds and facilities for our research.

References

[1] Parveez, K. A., Nur Nadia, K., Norliyana, Z. Z., Meilina, O., Rahwahwati, M. S. R., Loh, S. K., Kanga Rani, S., Hoong, S. S. and Zainab, I., (2022). Oil Palm Economic Performance in Malaysia and R&D Progress in 2021. *Journal Oil Palm Research,* Vol. 34, 185-218. https://doi.org/10.21894/jopr.2022.0036.

[2] Roslan, A. and Idris, A. S., (2012). Economic Impact of *Ganoderma* Incidence on Malaysian Oil Palm Plantation – A Case Study in Johor. *Oil Palm Industry Economic Journal,* Vol.12, 24-30.

[3] Idris, A. S., Mazliham, M. S., Loonis, P. and Basri, W., (2010a). GanoSken for Early Detection of *Ganoderma* Infection in Oil Palm. *MPOB Information Series,* Vol. 442, 1-4.

[4] Idris, A. S., Rajinder, S., Madihah, A. Z. and Basri, M. W., (2010b). Multiplex PCR-DNA Kit for Early Detection and Identification of *Ganoderma* Species in Oil Palm. *MPOB Information Series,* Vol.73, 1-4.

[5] Ariffin, D. and Idris, A. S., (1992). The *Ganoderma* Selective Medium (GSM). *MPOB Information Series,* Vol. 8, 1-2.

[6] Izzuddin, M. A., (2010). *Early Detection of Ganoderma Disease in Oil Palm using Field Spectroscopy*. MSc Thesis, Universiti Putra Malaysia, 130.

[7] Izzuddin, M. A., Idris, A. S., Nisfariza, M. N., Nordiana, A. A., Shafri, H. Z. M. and Ezzati, B., (2017). The Development of Spectral Indices for Early Detection of *Ganoderma* Disease in Oil Palm Seedlings. *International Journal Remote Sensing,* Vol. 38, 6505-6527. https://doi.org/10.1080/01431 161.2017.1335908.

[8] Shafri, H. Z. M. and Yusof, R., (2009). Determination of Optimal Wavelet Denoising Parameters for Red Edge Feature Extraction from Hyperspectral Data. *Journal of Applied Remote Sensing,* Vol. 3(1), https://doi.org/10. 1117/1.3155804.

[9] Jardim, R. and Morgado-Dias, F., (2020). Savitzky–Golay Filtering as Image Noise Reduction with Sharp Colour Reset. *Microprocessors and Microsystems,* Vol.74. https://doi.org/10.1016/j.micpro.2020.103006.

[10] Resonon, (2021). Hyperspectral Software: Spectronon Pro: https://resonon.com/software, [Accessed Dec. 30 2021].

[11] Mathworks., (2021). Optimised Discriminat Analysis. https://www.mathworks.com/help/ stats/classification.html?s_tid=C RUX_lftnav. Accessed Dec. 30 2021].

ISSN: 1686-6576 (Printed) | ISSN 2673-0014 (Online) | © Geoinformatics International